

Peierls phonons in organic molecular crystals and in charge transfer salts

ALBERTO GIRLANDO^{1*}, MATTEO MASINO¹, ALDO BRILLANTE²,
RAFFAELE G. DELLA VALLE², ELISABETTA VENUTI²

¹ Dip. Chimica G.I.A.F. and INSTM-UdR Parma, Parma University, Parma, Italy

² Dip. Chimica Fisica ed Inorg. and INSTM-UdR Bologna, Bologna University, Italy

We review the Quasi-Harmonic Lattice Dynamic (QHLD) method, which we have recently implemented and adopted to carefully reproduce the crystal structure and lattice phonon dynamics of molecular crystals as a function of temperature and pressure. Association with mean field electronic structure calculations allows us to characterize the Peierls coupling, namely the coupling between electrons and lattice phonons. We apply this method to organic superconductors based on bis-ethylene-dithio-tetrathiafulvalene (BEDT-TTF), showing that many experimental findings related to superconducting properties are rationalized in terms of the Peierls coupling. Electron–intramolecular phonon coupling and electron–electron interactions, however, have to be taken into account for a full characterization. We also present results concerning another class of molecular crystals, the acenes. In this case, the focus is on the understanding of the temperature dependences of mobilities. First and foremost, however, we emphasize the possibility of accurately predicting both the crystal structure and lattice phonon spectral signatures. We analyse pentacene and tetracene, showing that both systems can crystallize into two different polymorphs. The two polymorphs have comparable stabilities, and can coexist in the same crystallite. Raman spectroscopy in the lattice phonon region is used as a convenient tool to identify the two phases. The Peierls coupling strength of pentacene is evaluated.

Key words: *electron-phonon coupling; lattice phonons; organic superconductors; acenes*

1. Introduction

The coupling between electrons and intermolecular (lattice) phonons, or the Peierls coupling, is at the heart of many fundamental phenomena in low-dimensional molecular crystals. Yet the role of Peierls phonons in basic properties such as charge transport has to be clarified. We have recently implemented [1, 2] a method (Quasi

*Corresponding author, e-mail: alberto.girlando@unipr.it.

Harmonic Lattice Dynamics – QHLD) able to accurately reproduce the crystal structure and lattice phonon dynamics of complex molecular crystals, also as a function of temperature and pressure. Association with Raman measurements and mean field electronic structure calculations allows one to characterize the phonon structure and the corresponding Peierls coupling. Here, we describe the successful application of the model to two rather different classes of molecular crystals, bis-ethylene-dithio-tetrathiafulvalene (BEDT-TTF) superconductors and acene semiconductors.

2. The QHLD method

In our approach, we start from the isolated molecule, using standard DFT methods (6-31G(d) basis, B3LYP hybrid functional) to calculate the molecular geometry, atomic charges, vibrational frequencies and Cartesian eigenvectors of the normal modes. These data are used to deal with molecular degrees of freedom when considering the molecular crystal. The intermolecular potential energy Φ_{inter} in the molecular crystal is expressed in terms of an atom–atom Buckingham model, combined with an electrostatic contribution represented by the set of DFT (ESP) atomic charges q_m calculated for the isolated molecule [1, 2]:

$$\Phi_{\text{inter}} = \frac{1}{2} \sum_{mn} \left[A_{mn} \exp(-B_{mn} r_{mn}) - \frac{C_{mn}}{r_{mn}^6} + \frac{q_m q_n}{r_{mn}} \right] \quad (1)$$

where the sum extends over all distances r_{mn} between pairs m, n of atoms in *different* molecules. The Ewald method is used to accelerate the convergence of the Coulomb interaction $q_m q_n / r_{mn}$. A_{mn} , B_{mn} , and C_{mn} in the Buckingham part of the potential are empirical atomic parameters – there is one triad for each different pair of atoms involved. The Buckingham parameters should be, in principle, universal parameters, transferable among different crystals containing the same atoms. In practice, they are transferable only within the class of molecular crystals they have been tuned for.

Given the above atom–atom potential, the effect of temperature T and pressure p are accounted for by computing the structure that has minimum Gibbs energy $G(p, T)$ with the QHLD method. In this method, where the vibrational Gibbs energy of the phonons is estimated in the harmonic approximation, the Gibbs energy of the system is expressed as:

$$G(p, T) = \Phi_{\text{inter}} + pV + \sum_{\mathbf{q}, j} \left\{ \left(\frac{\hbar v_{\mathbf{q}, j}}{2} \right) + k_B T \ln \left[1 - \exp(-\hbar v_{\mathbf{q}, j} / k_B T) \right] \right\} \quad (2)$$

where V is the molar volume, $\sum_{\mathbf{q}, j} (\hbar v_{\mathbf{q}, j} / 2)$ is the zero-point energy, and the last term is the entropic contribution of the lattice phonons. The sums extend over all j phonon branches of frequency $v_{\mathbf{q}, j}$ and wave vector \mathbf{q} . Given an initial lattice structure, one

computes Φ_{inter} and its derivatives with respect to the molecular coordinates. The second derivatives form the dynamical matrix, which is diagonalised to yield the lattice phonon frequencies and eigenvectors. The structure as a function of T and p is then obtained by minimizing $G(T,p)$ with respect to the lattice parameters, molecular positions and orientations.

In the above expressions, the lattice phonons are considered separately from molecular vibrations. This is the so-called rigid molecule approximation, but in crystals made up of large molecules the approximation is no longer valid, and there is a certain amount of coupling between lattice and low-frequency intramolecular phonons. To account for such a coupling, we adopt an exciton-like approach [3], where the interaction between different molecular coordinates is mediated by the intermolecular potential depending on atomic displacements. These correspond to the Cartesian eigenvectors of the isolated molecule normal modes calculated by DFT.

3. The Peierls coupling strength

The QHLD method provides a rather accurate description of the lattice phonon frequencies and eigenvectors, independent of the crystal electronic structure. In order to evaluate the strength of the Peierls coupling, we also need a proper description of the electronic degrees of freedom, which is not a trivial problem in the case of molecular crystals, as they are characterized by narrow bands and strong electronic correlations. Coherently with the QHLD scheme, we adopt a semi-empirical approach, which is less computer demanding and gives a better insight into the type of lattice phonons involved in the Peierls coupling. We define the Peierls, or electron–lattice phonon (e-LP), coupling constants $g(KL; \mathbf{q}, j)$ as:

$$g(KL; \mathbf{q}, j) = \left(\frac{\partial t_{KL}}{\partial Q_{\mathbf{q}j}} \right)_0 \quad (3)$$

where t_{KL} is the hopping or charge-transfer (CT) integral between neighbouring pairs of molecules KL and $Q_{\mathbf{q}j}$ is the dimensionless normal coordinate for the j th phonon with the wave vector \mathbf{q} . In this definition, the electronic part is dealt with in real space, being relevant to a pair of molecules: the CT integrals are indeed calculated as the variation of the HOMO (LUMO) energy in going from an isolated molecule to the KL pair. The HOMO (LUMO) energy and its $Q_{\mathbf{q}j}$ modulation is computed by an appropriate semi-empirical method, such as the extended Hückel (EH) [4] or the ZINDO methods [5]. Even then, the computational effort is considerable, given the high number of vibrational degrees of freedom. On the other hand, the coupling constants of optical phonons depend weakly on the phonon wave vector, so we evaluate them only at $\mathbf{q} = 0$. The coupling constants of acoustic phonons are zero by symmetry at the zone centre; therefore, we calculate them at several representative zone-border points and

assume a linear dependence of $g^2(j)/v_j$ on $|\mathbf{q}|$. An appropriate tight binding scheme is adopted to compute the band structure starting from the value t for the nearest neighbours, and to evaluate the dependence of the coupling constants from the electronic wave vector \mathbf{k} [2].

4. Raman measurements

Raman spectra have been collected with a Jobin Yvon T64000 spectrometer, coupled to an Olympus microscope, with a spatial resolution between 2 and 1 μm , yielding the possibility of spatially mapping the crystals under investigation. Exciting lines were from a Krypton ion laser. Micro-Raman measurements at low temperatures (down to 80 K) and high pressures (up to 6 GPa) have been performed with a liquid Nitrogen Linkam HFS 91 cryostat and with a LOTO diamond anvil cell, respectively. Both were mounted on the microscope stage.

5. BEDT-TTF superconductors

The nature of the pairing mechanism in superconducting BEDT-TTF salts has been the subject of extensive discussions [6]. The superconducting state is adjacent to magnetically or charge ordered states, showing evidence of important electron-electron interactions. On the other hand, the crystal and phonon structures of these salts are very complex, so the possible role of phonons in the superconductivity mechanism is difficult to assess. We have applied the QHLD method to $(\text{BEDT-TTF})_2\text{I}_3$ salts [7, 8], which have several non-superconducting and superconducting phases. We have verified that the various phases indeed correspond to minima of the Gibbs energy. The available experimental data (Raman, specific heat) connected to the lattice phonons of the superconducting β^* - and κ -phases are properly reproduced. The Peierls coupling constants have been evaluated by the EH tight-binding scheme, within the framework of the dimer model [2].

By expressing the Peierls coupling constants in the reciprocal space, we evaluate the Eliashberg function, which turns out to be in a qualitative agreement with available β^* - and κ - $(\text{BEDT-TTF})_2\text{I}_3$ experimental data. From the Eliashberg function, we derive the dimensionless coupling constant λ and the logarithmic average phonon frequency ω_n . When these quantities are substituted in the Allen-McMillan equation for the superconducting T_c [9], we find values well below the experimental ones. The values of T_c depend critically on the electronic density of states at the Fermi energy $N(E_F)$, which is difficult to evaluate. In any case, the Peierls coupling does not account for β^* - and κ - $(\text{BEDT-TTF})_2\text{I}_3$ values of T_c . The above scenario changes substantially when we include the Holstein (electron–intramolecular) coupling when evaluating λ and ω_n . Indeed, Holstein coupling contributes to λ in only about 25%, but ω_n is

more than doubled. Then, even before trying to estimate the superconducting critical temperature, it is instructive to see if the new value of ω_n including the Holstein (intramolecular) contribution accounts for other experimental observables related to superconductivity. Indeed, some years ago Marsiglio and Carbotte [10] proposed empirical relations directly connecting ω_n to the superconducting gap Δ_0 and to the specific heat jump at T_c . Table 1 shows that there is an excellent agreement between experiment and the values estimated through the Marsiglio and Carbotte relations. Finally, by assuming plausible values for $N(E_F)$, the Allen–McMillan equation gives the values of T_c in agreement with experiment and properly scaled for the two salts [7, 8].

Table 1. Calculated and experimental superconducting gap, $2\Delta_0$, and specific heat jump, $\Delta C_p/\gamma T_c$, of two superconducting (BEDT-TTF)₂I₃ salts

Superconducting phase	$2\Delta_{0\text{CALC}}$ (cm ⁻¹)	$2\Delta_{0\text{EXP}}$ (cm ⁻¹)	$(\Delta C_p/\gamma T_c)_{\text{CALC}}$	$(\Delta C_p/\gamma T_c)_{\text{EXP}}$
β^* (BEDT-TTF) ₂ I ₃	22	25 ^a	–	–
κ -(BEDT-TTF) ₂ I ₃	9	12 ^b	1.7	1.6 ^c

^afrom Ref. [11].

^bFrom Ref. [12].

^cFrom Ref. [13].

As a further test of our approach, we have considered the effect of pressure on T_c . In BEDT-TTF salts, the decrease of T_c with p is large, up to ~ 3 K/kbar [14]. This unusual pressure effect has been sometimes taken as the evidence of a non-conventional pairing mechanism [15]. We have calculated the crystal and lattice phonon structure of β^* -(BEDT-TTF)₂I₃ at 8 K, under 0 and 6 kbars. The pressure effect on the Holstein coupling is very small, and has been disregarded. Preliminary results show that the calculated decrease in T_c is smaller than that measured (about 1 K vs. almost 5 K). Even keeping in mind all the approximations of the calculations, which are currently being refined and checked, we underline that the Peierls variation with p is at least as important as the variation in $N(E_F)$. From the data presented above, we conclude that the phonon contribution cannot be disregarded in a proper description of the coupling mechanism in organic superconductors.

6. Acene semiconductors

Acene crystals exhibit the highest mobilities among organic semiconductors [16], and the Peierls coupling is thought to be important in explaining the temperature dependence and anisotropy of the mobilities [17]. On the other hand, for practical applications at room temperature, it is much more important to assess the acene crystal structures and the corresponding lattice phonon spectral signatures. Indeed, the polymorphism of pentacene has been the subject of intense experimental and theoretical studies [18].

By applying our computational method, we have first aimed to identify the genuinely different polymorphs among the various reported single-crystal X-ray structures. We have obtained two local minima of the potential energy Φ_{inter} , i.e., two different “inherent structures” [19]. This behaviour clearly indicates that there are at least two different single crystal polymorphs of pentacene. One of them (polymorph C) corresponds to the structure reported in 1962 by Campbell and Robertson [20]. The other (polymorph H) corresponds to the structure found in all more recent measurements [21]. We have also obtained information on the global stability of the minima by systematically sampling the potential energy surface, and have found that the two polymorphs correspond to the two deepest minima [22]. The calculations also predict significant differences between the corresponding Raman spectra that we have checked experimentally, confirming the existence of two polymorphs [23]. Micro-Raman measurements have also shown that the two polymorphs can coexist as micro-domains in the same crystal. Application of pressures beyond 0.6 GPa irreversibly transforms polymorph C into the thermodynamically more stable H phase [24].

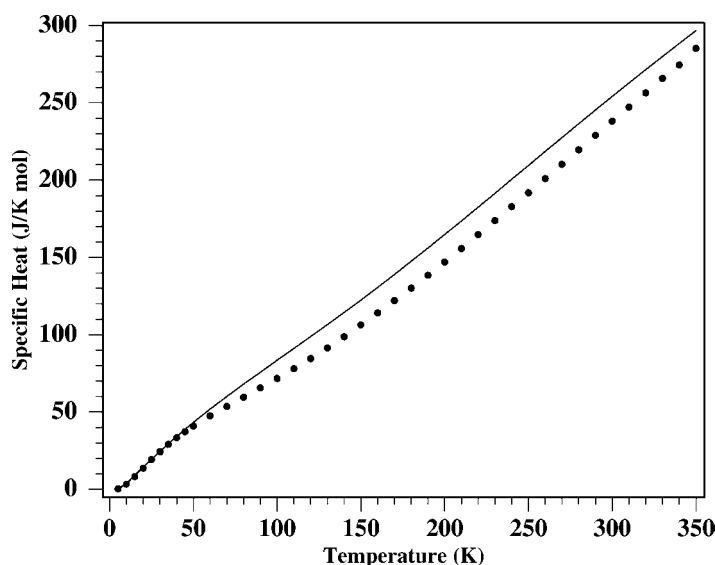


Fig. 1. Temperature dependence of tetracene specific heat.
Dots: experiment (from Ref. [26]); continuous line: QHLD calculations

Only one complete X-ray crystal structure has been reported for tetracene [20], which is known to undergo a phase transition both when lowering T and increasing p [25]. No clear indications exist about the low T and high p structures, partly because the crystal is damaged upon the phase transition. Our combination of theoretical and spectroscopic approaches is the key in elucidating this case. First, we have explored the potential energy surface of tetracene, finding that, similarly to pentacene, there are two minima very close in energy, one of which corresponds to the room temperature

experimental crystal structure. The calculated thermodynamic properties of the two polymorphs are very similar – the experimental temperature dependence of the specific heat [26], which is calculated very well by our model (Fig. 1), indeed does not show evidence of phase transitions. On the other hand, the QHLD method predicts that Raman lattice mode frequencies should be different for the two polymorphs. Raman spectra as a function of T gave evidence for a phase transition from one polymorph to the other below 135 K. We have shown that the same low-temperature polymorph can also be obtained by applying pressure [25].

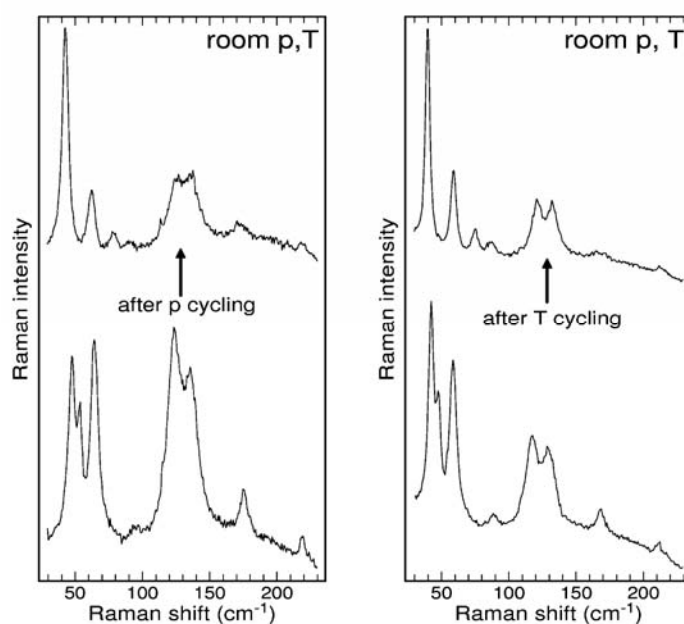


Fig. 2. Raman spectra of tetracene in the lattice phonon frequency region at ambient conditions. Bottom spectra: as grown crystals. Top spectra: after undergoing the T -induced (left) and the p -induced (right) phase transitions

As shown in Fig. 2, transitions induced by both T and p show large hysteresis or even irreversibility, so that the initial phase is not recovered when the sample is brought back to ambient conditions. The ambient tetracene polymorph has a crystal structure very similar to the C phase of pentacene, whereas the low T , high p phase is similar to the denser phase H. As in the case of pentacene, micro-Raman spectroscopy reveals phase inhomogeneities that might affect tetracene mobilities. The lattice phonon Raman spectroscopy therefore represents a convenient and reliable tool for checking crystal quality, providing a way to improve the performance of acene-based devices.

In the case of pentacene, we have also started to evaluate the strength of the Peierls coupling. The Peierls coupling constants for $\mathbf{q} = 0$ optical phonons of pentacene have been computed as described above. Since pentacene has a simpler molecu-

lar structure than BEDT-TTF, we preferred the ZINDO to the EH method to evaluate the hopping integrals in this case. Table 2 reports the Valence (VB) and Conduction Band (CB) lattice relaxation energy, $E_{LR}(j)$, for the low-frequency lattice optical phonons of the pentacene H phase at 0 K. The lattice relaxation energy directly expresses the strength of the Peierls coupling and is defined as $E_{LR}(j) = G_j^2/2\pi\nu_j$, where G_j is the total Peierls coupling constant of mode j , a sum of the modulations of the four main hopping integrals in the ab crystal plane. By symmetry, only totally symmetric (A_g) phonons can be coupled to electrons. Table 2 shows that several phonons are appreciably coupled to the charge carriers, and that some difference exists between coupling in the VB and CB. Phonons above 203 cm^{-1} are not appreciably coupled, and the largest contribution ($\sim 70\%$) to the total lattice relaxation energy comes from the two lowest frequency modes, which are described as librations around the two short molecular axes approximately parallel to the conducting ab crystal plane. Given the low frequency of these librations, they are likely to affect the mobilities even at low temperatures. A more detailed analysis of pentacene and tetracene mobilities and their temperature dependences is in progress.

Table 2. Low-frequency A_g phonons and lattice relaxation energy E_{LR} of pentacene (H phase) at 0 K

$\nu (\text{cm}^{-1})$	Valence band $E_{LR} (\text{meV})$	Conduction band $E_{LR} (\text{meV})$
27	20.1	15.5
61	6.7	3.2
70	~ 0	1.1
96	1.2	2.5
132	~ 0	~ 0
148	2.6	~ 0
156	0.8	1.8
162	~ 0	~ 0
203	2.1	1.2

6. Conclusions

We have shown that the QHLD method can be employed to characterize the structure and lattice phonon dynamics of complex molecular crystals. The method is very simple, and its semi-empirical nature requires careful tuning over the class of molecular crystals of interest. In this way, a proper choice of parameters may compensate for the inherent approximations and shortcomings. The QHLD approach allows one to exploit the molecular nature of the crystals, dealing separately with the inter- and intramolecular phonon dynamics, the latter being solved through conventional *ab initio* methods. Association with mean-field electronic structure calculations has allowed us to characterize the Peierls coupling in two rather different classes of molecu-

lar crystals, BEDT-TTF organic superconductors and acene semiconductors. We have shown that the Peierls coupling plays a fundamental role in the superconducting pairing mechanism. In acene semiconductors, on the other hand, the QHLD method has provided important clues about the obtainable crystal phases, revealing the possible influence of crystal phase purity on the observed mobilities.

Acknowledgements

Work supported by the Consorzio Interuniversitario per la Scienza e Tecnologia dei Materiali (I.N.S.T.M. - PRISMA 2002 project) and by the Italian Ministry of University and Research (M.I.U.R. - FIRB 2003 project).

References

- [1] DELLA VALLE R.G., VENUTI E., FARINA L., BRILLANTE A., *Chem. Phys.*, 273 (2001), 197.
- [2] GIRLANDO A., MASINO M., VISENTINI G., DELLA VALLE R.G., BRILLANTE A., VENUTI E., *Phys. Rev.*, B62 (2000) 14476.
- [3] CALIFANO S., SCETTINO V., NETO N., *Lattice Dynamics of Molecular Crystals*, Springer-Verlag, Berlin, 1981.
- [4] HOFFMANN R., *J. Chem. Phys.* 39 (1965), 1397.
- [5] ZERNER M.C., LOEW G.H., KIRCHNER R.F., MUELLER-WESTERHOFF U.T., *J. Am. Chem. Soc.*, 102 (1980), 589.
- [6] LANG M., MUELLER J., [in:] K.H. Bennemann, J.B. Ketterson (Eds.), *The Physics of Superconductors*, Vol. 2, Springer-Verlag, Heidelberg, 2003.
- [7] GIRLANDO A., MASINO M., BRILLANTE A., DELLA VALLE R.G., VENUTI E., *Phys. Rev.*, B66 (2002), 100507 (R).
- [8] GIRLANDO A., MASINO M., BRILLANTE A., DELLA VALLE R.G., VENUTI E., [in:] R.W. Stevens (Ed.), *New Developments in Superconductivity Research*, Nova Science Publishers, Hauppauge, 2003, p. 15.
- [9] ALLEN P.B., DYNES R.C., *Phys. Rev.*, B12 (1975), 905.
- [10] MARSIGLIO F., CARBOTTE J.P., *Phys. Rev.*, B 33 (1986), 6141.
- [11] DRICHKO N., HAAS P., GORSHUNOV B., SCHWEITZER D., DRESSEL M., *Europhys. Lett.*, 59 (2002), 774.
- [12] LUDWIG T., SCHWEITZER D., KELLER H.J., *Synth. Metals*, 85 (1985), 1587.
- [13] WOSNITZA J., LIU X., SCHWEITZER D., KELLER H., *Phys. Rev.*, B 50 (1994), 12747.
- [14] SADEWASSER S., LOONEY C., SCHILLING J.S., SCHLUETER J.A., WILLIAMS J.M., NIXON P.G., WINTER R.W., GARD G.L., *Solid State Comm.* 104 (1997), 571.
- [15] CAUFIELD J., LUBCZYNSKI W., PRATT F.L., SINGLETON J., KO. D.J.K., HAYES W., KURMOO M., DAY P., *J. Phys. C : Condens. Matter* 6 (1994), 2911.
- [16] DIMITRAKOPOULOS C.D., MASCARO D.J., *IBM Res. & Dev.*, 45 (2001), 11.
- [17] HANNEWALD K., BOBBERT P.A., *Phys. Rev.*, B69 (2004), 075212.
- [18] DELLA VALLE R.G., VENUTI E., FARINA L., BRILLANTE A., MASINO M., GIRLANDO A., *J. Phys. Chem.*, B 108 (2004), 1822, and references therein.
- [19] VENUTI E., DELLA VALLE R.G., BRILLANTE A., MASINO M., GIRLANDO A., *J. Amer. Chem. Soc.*, 124 (2002), 2128.
- [20] CAMPBELL R.B., ROBERTSON J.M., *Acta Cryst.*, 15 (1962), 289.
- [21] HOLMES D., KUMARASWAMY S., MATZGER A.J., VOLLHARDT K.P., *Chem.Eur.J.*, 5 (1999), 3399; SIEGRIST T., KLOC CH., SCHOEN J.H., BATTLOGG B., HADDON R.C., BERG S., THOMAS G.A., *Angew. Chem. Int. Ed. Engl.*, 40 (2001), 1732; MATTHEUS C.C., DROS A.B., BAAS J., MEETSMA A., DEBOER J.L., PALSTRA T.T.M., *Acta Cryst.*, C 57 (2001), 1732.

- [22] DELLA VALLE R.G., VENUTI E., BRILLANTE A., GIRLANDO A., J. Chem. Phys. 118 (2003), 807.
- [23] BRILLANTE A., DELLA VALLE R.G., FARINA L., GIRLANDO A., MASINO M., VENUTI E., Chem. Phys. Lett. 357 (2002), 32.
- [24] FARINA L., BRILLANTE A., DELLA VALLE R.G., VENUTI E., AMBOAGE M., SYASSEN K., Chem. Phys. Lett. 375 (2003), 490.
- [25] VENUTI E., DELLA VALLE R.G., FARINA L., BRILLANTE A., MASINO M., GIRLANDO A. Phys. Rev. B 70 (2004), 104106.
- [26] WONG W.K., WESTRUM JR.E.F., Mol. Cryst. Liq. Cryst. 61 (1980), 207.

Received 14 September 2004

Revised 2 November 2004